PHYSICAL REVIEW E **89**, 061101(R) (2014)

Comparisons of dense-plasma-focus kinetic simulations with experimental measurements

A. Schmidt,[1] A. Link,[1] D. Welch,[2] J. Ellsworth,[1] S. Falabella,[1] and V. Tang[1]
[1]*Lawrence Livermore National Laboratory, Livermore, California 94550, USA*
[2]*Voss Scientific, LLC, Albuquerque, New Mexico 87108, USA*
(Received 7 March 2014; published 26 June 2014)

Dense-plasma-focus (DPF) Z-pinch devices are sources of copious high-energy electrons and ions, x rays, and neutrons. The mechanisms through which these physically simple devices generate such high-energy beams in a relatively short distance are not fully understood and past optimization efforts of these devices have been largely empirical. Previously we reported on fully kinetic simulations of a DPF and compared them with hybrid and fluid simulations of the same device. Here we present detailed comparisons between fully kinetic simulations and experimental data on a 1.2 kJ DPF with two electrode geometries, including neutron yield and ion beam energy distributions. A more intensive third calculation is presented which examines the effects of a fully detailed pulsed power driver model. We also compare simulated electromagnetic fluctuations with direct measurement of radiofrequency electromagnetic fluctuations in a DPF plasma. These comparisons indicate that the fully kinetic model captures the essential physics of these plasmas with high fidelity, and provide further evidence that anomalous resistivity in the plasma arises due to a kinetic instability near the lower hybrid frequency.

DOI: 10.1103/PhysRevE.89.061101 PACS number(s): 52.58.Lq, 52.59.Hq, 52.65.Rr, 52.70.Gw

I. INTRODUCTION

We describe here three fully kinetic dense-plasma-focus (DPF) [1–4] simulations and compare their predictions in detail with a variety of measurements. These simulations remain stable and energy conserving through the entire Z-pinch phase, in which the plasma changes rapidly and exhibits high gradients. Modeling the entire Z-pinch phase—and thus counting all neutrons produced—is important for comparing yield predictions across different simulations. The production of a stable simulation for a specific configuration typically requires >100 000 CPU hours. Here we compare simulated and experimentally measured neutron yields for two DPF gun geometries, demonstrating the model's ability to distinguish performance between similar gun designs. We additionally show a third calculation in which the boundary condition between electrodes is modeled using a pulsed power circuit, in order to include driver effects in the calculation. The simulations shown here reproduce experimentally measured ion beam energy distributions and radiofrequency fields in the plasma. This is a comprehensive comparison of a fully kinetic model with these measured quantities in a DPF, demonstrating that the model can be used as a predictive design tool.

A DPF Z pinch is a device consisting of two coaxially located electrodes with a high-voltage source at one end (Fig. 1). In the presence of a low-pressure gas, the high-voltage source induces a surface flashover and the formation of a current-conducting plasma sheath across an insulator at the upstream end of the DPF. During the "run-down" phase, the current sheath is accelerated down the length of the electrodes by magnetic pressure, ionizing and sweeping up neutral gas as it accelerates. When the plasma sheath reaches the end of the inner electrode, a portion is pushed radially inward during the "run-in" phase. When the leading edge of the current sheath reaches the axis, it "pinches" the plasma to create a hot, dense region that emits high-energy electron and ion beams, x rays, and (in the presence of D or D-T) neutrons [4].

In addition to fluid modeling of DPFs, previous modeling work has included a non-self-consistent test particle approach to look at kinetic effects [5–9], kinetic simulations of a Z pinch with scaled ion-electron mass ratio [10], and kinetic simulations of a conventional gas-puff Z pinch [11]. We previously reported on a fully kinetic model of a DPF Z-pinch device, including electrode boundaries, and demonstrated that a fully kinetic (both ions and electrons kinetic) approach is needed in order to see kinetic effects during the pinch phase, such as kinetic instabilities and beam formation [12]. Past measurements of DPF rf emission have been performed using microwave antennas in conjunction with bandpass waveguides that allowed various frequency bands to be transmitted [13].

II. SIMULATION AND EXPERIMENTAL SETUP

The simulation setup is detailed in [12] and is briefly summarized here: Calculations were performed in the particle-in-cell (PIC) code large scale plasma (LSP) [14]. The time step was varied from 2.5×10^{-4} to 8×10^{-6} ns, and was reduced as the magnetic field in the simulation increased, ensuring the resolution of the electron cyclotron frequency. The calculation is initialized at the end of the run-down phase, with a 1-mm-width plasma sheath of uniform density. The neutral gas density in front of the sheath corresponds to 1 Torr at STP, and the region behind the sheath is initially vacuum. The sheath density corresponds to a 10% sweepup of neutral gas during the run-down.

Simulations are two dimensional in cylindrical coordinates (r,z). The two simulated electrode geometries shown in Fig. 2 correspond to experimental geometries used on the existing 1.2 kJ DPF at Lawrence Livermore National Laboratory (LLNL) [15]. The cathodes (outer electrodes) are represented by conducting boundaries at $r = 1.5$ cm and $r = 3.0$ cm for the two geometries. In the experiment, the cathode is not cylindrically symmetric, as it is a set of eight rods arranged in a circular pattern. A 5-cm-long anode is represented by a conductive cylinder with outer radii of 1 and 1.5 cm for the two geometries. In the smaller geometry, the anode is hollowed out, while the larger geometry has only a small depression in the anode (Fig. 2).

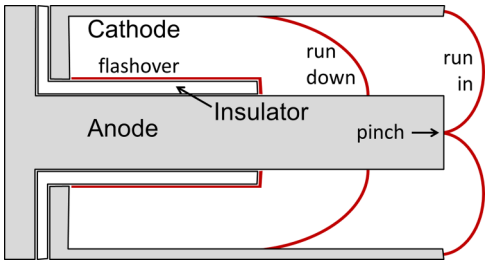

FIG. 1. (Color online) Schematic of a dense-plasma-focus Z pinch, including flashover, run-down, run-in, and pinch. The plasma sheath is shown in red (dark gray).

The voltage drive is modeled here in two ways. The first, and less computationally expensive, is with a prescribed incoming voltage wave traveling the length of the anode, with a reflected wave traveling back. The voltage is ramped up during the first 10 ns of the simulation (before the run-in), and then kept constant for the remainder of the simulation, resulting in a steady-state current of 180 and 200 kA, for the small and large guns, respectively (Fig. 3), before the pinch.

An additional simulation was run for the larger gun geometry which included the details of the driver characteristics, including capacitance, resistance, inductance, and line impedance. Using this driver model requires that the simulation run for ~450 ns of the circuit rise in addition to the ~160 ns of run-in and pinch (Fig. 3). To keep the simulation manageably sized, the particles were initially placed at the end of the run-down and prevented from moving while the transmission line current rose nearly to its peak value. This method requires more computing time than the voltage wave method, but allows for self-consistent modeling of the plasma and drive after the particles are permitted to move.

While past DPF circuit models could predict the effect of driver characteristics on general plasma properties such as sheath speed, this model self-consistently predicts neutron yields including driver effects. Hereafter it can be used as a tool to predict and understand the performance for different drivers, such as the high-impedance drivers that have empirically been shown to increase DPF neutron yield [16–18].

The ion energy distributions inside our DPF were measured with a time-of-flight (TOF) Faraday Cup diagnostic (Kimball

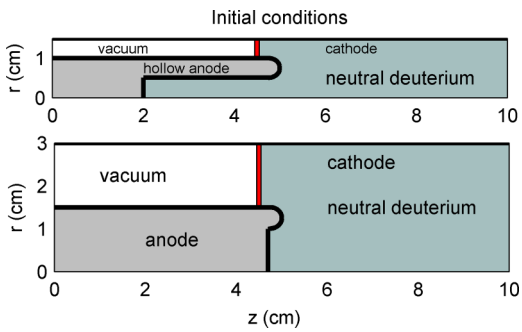

FIG. 2. (Color online) Initial conditions for simulations of the two experimentally tested DPF guns. Plasma sheath of both ions and electrons is centered at $z = 4.5$. The region behind the sheath is vacuum. In front of the sheath is neutral deuterium gas.

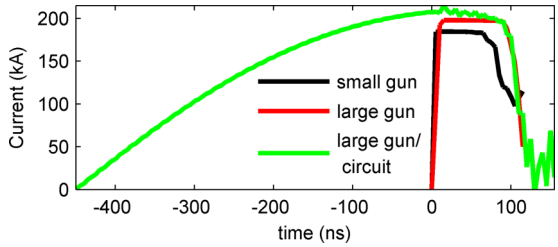

FIG. 3. (Color online) Simulated plasma current as a function of time. The time at which particles are allowed to move is marked as $t = 0$. Minor current oscillations in the pulsed-power-circuit simulation appear when the particles are allowed to move, after the current has ramped up to its maximum value.

Physics model FC-73A) located 65 cm from the pinch [15]. Neutron yields were measured with a helium-3 neutron detector, calibrated with a californium-252 source and accompanying Monte Carlo N-Particle code (MCNP) calculations [15]. The electric field oscillations were measured using a small rf pickup probe placed between cathode rods at the end of the anode, slightly inside the plasma. The rf probe was connected to a 12 GS/s oscilloscope for measurement of oscillations up to 5 GHz.

III. SIMULATION AND EXPERIMENTAL RESULTS

The kinetic simulations shown here remain stable and energy conserving through the entire pinch process so that a well-defined neutron yield could be obtained from specific electrode geometries (Fig. 4). Repeated calculations with identical plasma conditions but different gridding or time stepping exhibit a neutron yield variation of ~10%. The kinetic calculations were able to differentiate neutron yield between the two similar DPF electrode geometries that we have tested experimentally. The two voltage wave driver simulations predicted a yield of 2.8×10^7 with the smaller gun geometry (measured yields are up to 4×10^7) and 1.6×10^7 with the larger gun geometry (measured yields are up to 2×10^7), despite the current being higher in the larger gun simulation. It is encouraging that the predicted yields for two similar guns are correctly ranked, though a simulated pressure scan must be done to confirm this prediction.

Including the driver characteristics at the anode-cathode boundary has the effect of decreasing the time over which

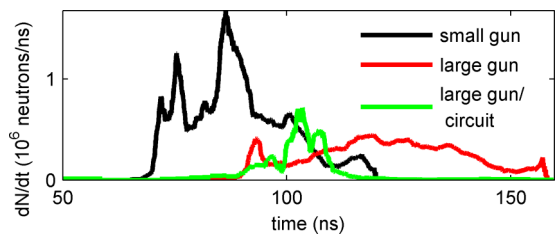

FIG. 4. (Color online) Simulated neutron production rate as a function of time. Calculations remain stable and energy conserving throughout the entire pinch until after neutron production stops, allowing us to compare simulated yields from multiple electrode geometries.

neutrons are produced (Fig. 4) and the overall yield. This result is expected since the real pulsed power system will not continue to provide a stiff voltage indefinitely. For the larger gun geometry with pulsed power circuit, a total yield of 6.9×10^6 was obtained, approximately half of the predicted yield when using the voltage wave driver. The neutron pulse was ~60 ns long with the voltage wave driver for both gun geometries and ~20 ns long with the pulsed power circuit. In both geometries, the simulations predict that the majority of neutrons are born in a region within 1 mm of the axis, and with an axial extent of ~1 and ~2.5 cm for the smaller and larger gun geometries, respectively [Figs. 5(a) and 5(b)]. The predicted neutron birth region is shorter when the pulsed power circuit is included [Fig. 5(c)].

Simulated and measured energy distributions of ion beams emitted from the DPF with smaller gun are shown in Fig. 6. Measured energy distributions have been obtained from TOF Faraday cup measurements, which show significant signal above the noise for D^+ energies of 300 keV and below. The Faraday cup is on axis in front of the anode and its aperture subtends a 0.2° half angle relative to the pinch. The simulated ion energy distribution was taken from a conic section with 22° half angle for sufficient particle statistics. Substantial agreement between the simulated and measured distributions

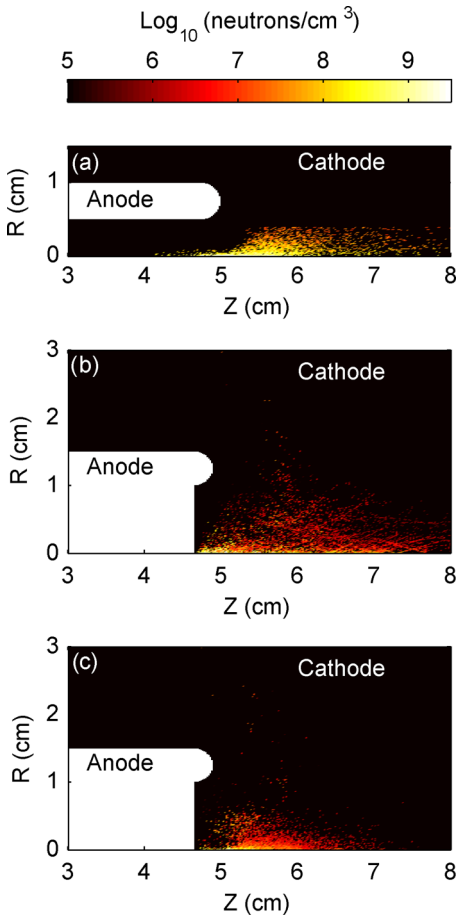

FIG. 5. (Color online) Log of neutron density at neutron birth location for (a) the smaller gun, (b) the larger gun, and (c) the larger gun with pulsed power circuit. The simulations predict that the majority of neutrons are born within 1 mm of the axis.

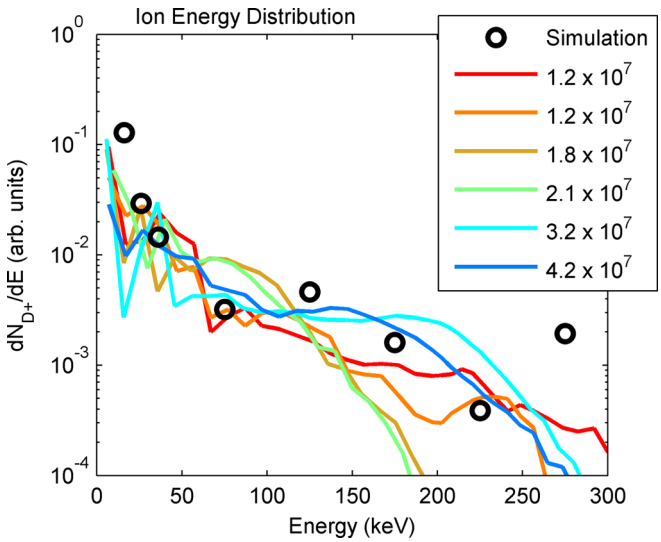

FIG. 6. (Color online) Simulated (black circles) and measured ion energy distributions for the smaller gun geometry. Shot yields are shown in the inset and vary from 1.2×10^7 to 4.2×10^7. Measured ion energy distributions have been obtained from time-of-flight Faraday cup measurements. In these shots, the Faraday cup signal is comparable to the noise for time-of-flight data corresponding to energies of ~300 keV and above.

is found under 300 keV. The simulations additionally show a small population of ions with energies up to 1 MeV. Ion beams have been observed on a variety of DPFs with energies up to 8 MeV [19,20], but MeV+ ions measured on other experiments are one to three orders of magnitude weaker in signal from 300 keV ions, and thus are not detectable with our experimental setup.

The frequency content of measured and simulated electromagnetic (EM) fields during the pinch for the larger gun geometry is shown in Fig. 7. An EM pickup probe positioned between cathode rods and connected to a high-bandwidth oscilloscope was used to measure EM oscillations in the plasma, up to 5 GHz. Figure 7(a) shows examples from both high- and low-quality pinches, as determined by the depth of the current dip and the neutron yield. Poor pinches did not exhibit fluctuations above 3 GHz, while high-quality pinches exhibited strong fluctuations in the 3–4 GHz range.

A synthetic E_z probe was placed in the simulated plasma, 0.75 cm from the axis. The synthetic probe from the pulsed-power-circuit simulation exhibited its strongest fluctuations in the 3–4 GHz range [Fig. 7(b)]. Additionally, the simulated probe predicted higher-frequency fluctuations that appear to be higher harmonics of the lower frequencies present. The two simulations with voltage wave driver also showed fluctuations in the same general frequency range, but with frequency peaks less aligned with the experimental data. This result may be expected, given that the rise of kinetic instabilities in the plasma could be heavily influenced by feedback from the driver. The simulations show fields of 10–40 T present for the entire pinch phase, corresponding to a lower hybrid frequency of ~4.6–18 GHz. The observed oscillations are close to this frequency range and far from other characteristic plasma and cyclotron frequencies, suggesting

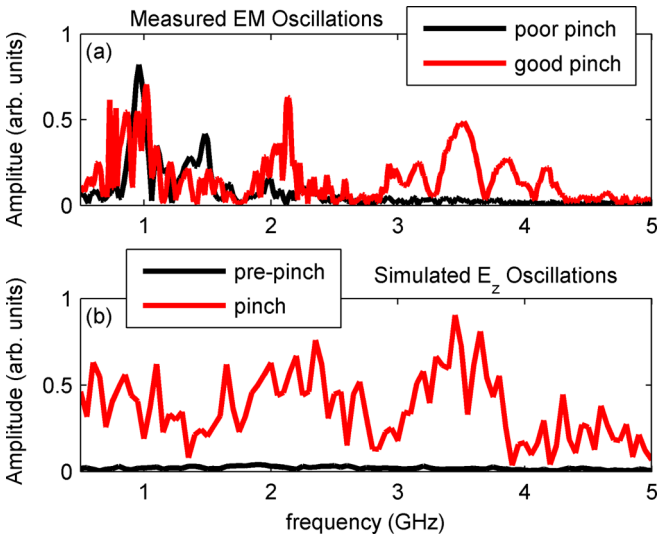

FIG. 7. (Color online) Frequency content of measured EM oscillations (a) and simulated E_z probe (b) for the larger electrode configuration with full pulsed power circuit. Measured oscillations above 3 GHz are only observed in "high-quality" pinches—those with large current dip and high neutron yield. Oscillations in the simulation are present during the pinch and for ~20 ns before the pinch. Both simulated and measured oscillations show activity in the 3–4 GHz range.

that the long-suspected lower hybrid drift instability may be present.

A time-dependent inductance for the gun and plasma was calculated in the pulsed-power-circuit simulation using the simulated magnetic energy and plasma current. The total inductance of the gun and plasma rises up to 10 nH during the ion beam formation and as high as 22 nH postpinch. The contribution from the gun alone is 7 nH. A time-dependent resistance of the plasma was then calculated by dividing the component of the voltage which is not due to $d(LI)/dt$ by the plasma current. The plasma resistance is between 0.2 and 2 Ω during the fast ion beam formation, and rises up to 3.5 Ω postpinch. The peak inductance and resistance values are higher than the 10–19 nH (7 nH gun+3–12 nH plasma) and 1–1.5 Ω that we have estimated in our experiment from current traces [15]. They originate from an unphysically large dip in the current postpinch. The current dip may be artificially high because the initialization of a vacuum region behind the sheath prevents a restrike from occurring in the anode-cathode gap in these simulations. Future work will address the fidelity of the simulations after the pinch, so that postpinch features such as restrikes and multiple pinches can be resolved.

Approximating the pinch plasma as a 1.1-cm-long by 0.75-mm-radius cylinder, a plasma resistance of 3.5 Ω implies a resistivity of 56 mΩ cm. If we instead assume that the resistivity is closer to 1 Ω, as inferred from our current traces, then the implied plasma resistivity is 16 mΩ cm. Classical resistivity from collisions and local plasma conditions in the pinch area is ~20 $\mu\Omega$ cm, about three orders of magnitude lower than the anomalous resistivity observed in the simulations and experiment. The ion beam does not begin to form in the simulation until the resistivity is >100× greater than classical values.

IV. SUMMARY

We have obtained simulated neutron yields and directly compared them with measured yields for two electrode geometries. The models with voltage wave driver predict neutron yields for the two geometries of 70%–80% of their maximum measured yields and correctly rank the yields of the two similar guns. Inclusion of the driver characteristics at the boundary condition lowers the predicted neutron pulse length and total yield. Substantial agreement in ion beam energy distributions is found. We have made direct measurements of electromagnetic oscillations in a DPF plasma using an EM pickup probe and shown that they exhibit similar frequency content to oscillations in simulated E_z fields. This correlation provides further evidence that a kinetic instability is responsible for pinch behavior and that fully kinetic simulations can reproduce this effect. This simulation capability is well benchmarked at the kJ DPF level and now can be used to guide design of DPF systems, including drivers.

ACKNOWLEDGMENTS

This work was performed under the auspices of the US Department of Energy by Lawrence Livermore National Laboratory (LLNL) under Contract No. DE-AC52-07NA27344 and was supported by the Laboratory Directed Research and Development Program (11-ERD-063) at LLNL. Computing support for this work came from the LLNL Institutional Computing Grand Challenge program.

[1] A. Bernard, H. Bruzzone, P. Choi, H. Chuaqui, V. Gribkov, J. Herrera, K. Hirano, A. Krejci, S. Lee, C. Luo, F. Mezzetti, M. Sadowski, H. Schmidt, K. Ware, C. S. Wong, and V. Zoita, J. Moscow Phys. Soc. **8**, 93 (1998).

[2] M. G. Haines, Plasma Phys. Controlled Fusion **53**, 093001 (2011).

[3] J. W. Mather, Phys. Fluids **7**, S28 (1964).

[4] J. W. Mather, Phys. Fluids **8**, 366 (1965).

[5] R. Deutsch, W. Kies, and G. Decker, Plasma Phys. Controlled Fusion **28**, 1823 (1986).

[6] S. P. Gary and F. Hohl, Phys. Fluids **16**, 997 (1973).

[7] M. G. Haines, Nucl. Instrum. Methods Phys. Res. **207**, 179 (1983).

[8] Y. Kondoh and M. Mamada, Phys. Fluids **29**, 483 (1986).

[9] V. Tang, M. L. Adams, and B. Rusnak, IEEE Trans. Plasma Sci. **38**, 719 (2010).

[10] T. Haruki, H. R. Yousefi, K. Masugata, J.-I. Sakai, Y. Mizuguchi, N. Makino, and H. Ito, Phys. Plasmas **13**, 082106 (2006).
[11] D. R. Welch, D. V. Rose, R. E. Clark, C. B. Mostrom, W. A. Stygar, and R. J. Leeper, Phys. Rev. Lett. **103**, 255002 (2009).
[12] A. Schmidt, V. Tang, and D. Welch, Phys. Rev. Lett. **109**, 205003 (2012).
[13] G. Gerdin, M. J. Tanis, and F. Venneri, Plasma Phys. Controlled Fusion **28**, 527 (1986).
[14] D. R. Welch, D. V. Rose, M. E. Cuneo, R. B. Campbell, and T. A. Mehlhorn, Phys. Plasmas **13**, 063105 (2006).
[15] J. L. Ellsworth, S. Falabella, V. Tang, A. Schmidt, G. Guethlein, S. Hawkins, and B. Rusnak, Rev. Sci. Instrum. **85**, 013504 (2014).
[16] G. Decker, W. Kies, M. Mälzig, C. van Calker, and G. Ziethen, Nucl. Instrum. Methods Phys. Res. A **249**, 473 (1986).
[17] W. Kies, Plasma Phys. Controlled Fusion **28**, 1645 (1986).
[18] G. Decker, W. Kies, and G. Pross, Phys. Fluids **26**, 571 (1983).
[19] W. H. Bostick, H. Kilic, V. Nardi, and C.W. Powell, Nucl. Fusion **33**, 413 (1993).
[20] R. L. Gullickson and H. L. Sahlin, J. Appl. Phys. **49**, 1099 (1978).